Journal of Biomechanics 47 (2014) 3162–3168

Contents lists available at ScienceDirect

Journal of Biomechanics

journal homepage: www.elsevier.com/locate/jbiomech
www.JBiomech.com

Countermovement strategy changes with vertical jump height to accommodate feasible force constraints

Seyoung Kim [a,*], Sukyung Park [b], Sangkyu Choi [a]

[a] Department of Robotics and Mechatronics, Korea Institute of Machinery & Materials (KIMM), Daejeon, South Korea
[b] Department of Mechanical Engineering, Korea Advanced Institute of Science and Technology (KAIST), Daejeon, South Korea

ARTICLE INFO

Article history:
Accepted 12 June 2014

Keywords:
Standing vertical jump
Countermovement
Push-off
Downward momentum
Force advantage

ABSTRACT

In this study, we developed a curve-fit model of countermovement dynamics and examined whether the characteristics of a countermovement jump can be quantified using the model parameter and its scaling; we expected that the model-based analysis would facilitate an understanding of the basic mechanisms of force reduction and propulsion with a simplified framework of the center of mass (CoM) mechanics. Ten healthy young subjects jumped straight up to five different levels ranging from approximately 10% to 35% of their body heights. The kinematic and kinetic data on the CoM were measured using a force plate system synchronized with motion capture cameras. All subjects generated larger vertical forces compared with their body weights from the countermovement and sufficiently lowered their CoM position to support the work performed by push-off as the vertical elevations became more challenging. The model simulation reasonably reproduced the trajectories of vertical force during the countermovement, and the model parameters were replaced by linear and polynomial regression functions in terms of the vertical jump height. Gradual scaling trends of the individual model parameters were observed as a function of the vertical jump height with different degrees of scaling, depending on the subject. The results imply that the subjects may be aware of the jumping dynamics when subjected to various vertical jump heights and may select their countermovement strategies to effectively accommodate biomechanical constraints, i.e., limited force generation for the standing vertical jump.

© 2014 Elsevier Ltd. All rights reserved.

1. Introduction

In the standing vertical jump, a countermovement is a preliminary downward action that flexes the knees and hips before shortening the muscles for upward motion (Linthorne, 2001). As reported previously, subjects are generally able to jump higher with the countermovement than without any counter action (e.g., squat jump) (Bobbert et al., 1996; Linthorne, 2001). The mechanisms responsible for the greater jump height have been widely discussed by various research groups in terms of simple kinematics and muscle physiology. Some authors argue that pre-stretching before muscle shortening allows the muscles to build up a high level active state, resulting in greater joint moments at the start of push-off (Bobbert et al., 1996; Van Schenau et al., 1997), while others suggest that the countermovement enables elastic energy storage and reutilization in the muscles and/or tendons for extra work (Anderson and Pandy, 1993; Komi, 2000; Svantesson et al., 1991). However, the exact cause of the force advantage of the countermovement remains to be clarified.

To better understand the comparative advantages of countermovement in terms of mechanics, the countermovement jump was directly compared with the squat jump (Linthorne, 2001; McLellan et al., 2011), which does not employ a preliminary downward phase and begins from a stationary semi-squatted posture instead of an upright standing posture. The force (i.e., ground reaction force)–displacement (i.e., displacement of center of mass) curves corresponding to the countermovement jump and the squat jump were plotted on the same graph and compared in terms of the work performed by the ground reaction force, which suggested that in the countermovement jump, the leg muscles attain a higher amount of vertical force across a wide range of vertical displacements before they begin to shorten.

Multiple approaches have been used in modeling studies of vertical jumping to understand the vertical jump strategy in terms of muscle coordination, muscle strength, and arm swing. The effects of ankle restriction (Arakawa et al., 2013) and trunk inclination (Vanrenterghem et al., 2008) on the coordination of vertical jumping were investigated in terms of the mechanical outputs, such as the maximum power and work. The role of the rate of force development on a vertical jump was tested during a countermovement jump to determine the relationship between the peak force and the vertical jump displacement (McLellan et al., 2011). The energetics and

* Corresponding author. Tel.: +82 42 868 7614.
E-mail address: seyoungkim@kimm.re.kr (S. Kim).

http://dx.doi.org/10.1016/j.jbiomech.2014.06.013
0021-9290/© 2014 Elsevier Ltd. All rights reserved.

benefits of the arm swing (Lees et al., 2006) and squat depth (Domire and Challis, 2007) in a maximal vertical jump were also investigated in terms of energy build-up and dissipation mechanisms.

Although several attempts have been made within a mechanical framework similar to the ones described above, to date, the countermovement dynamics have not been quantitatively explored using a descriptive mathematical model to understand the basic mechanisms of force reduction and propulsion while considering biomechanical constraints, i.e., the feasible force and the rate of force constraints.

There have been many recent studies concerning biomechanical constraints and postural strategies that have suggested that human movements, such as postural responses to external perturbations, are inevitably affected by biomechanical constraints. For example, the postural strategy changes from an ankle strategy to a hip strategy with increasing perturbation magnitudes of support translation (Horak and Nashner, 1986; Park et al., 2004) and forward push (Kim et al., 2012). Specifically, the hip joint torque increases with perturbation, while the ankle joint torque is more limited because of the maximum allowable joint torque. These continuous changes in postural responses have suggested that the central nervous system (CNS) uses a continuous representation of biomechanical constraints (Park et al., 2004).

In this study, we developed a curve-fit model of the countermovement dynamics and examined whether the characteristics of the countermovement jump can be quantified by the model parameter and its scaling. The trajectories of the vertical force were curve-fitted with a combination of a semi-sinusoidal waveform and a linear increase, and the model parameters were then examined as a function of the vertical jump height to study the change in jump strategies. This model-based analysis would facilitate an understanding of the basic mechanisms of force reduction and propulsion that concern the biomechanical constraints and jump strategies with a simplified framework of center of mass (CoM) mechanics and will allow the development of a realistic framework for multi-joint dynamics and/or muscle physiology.

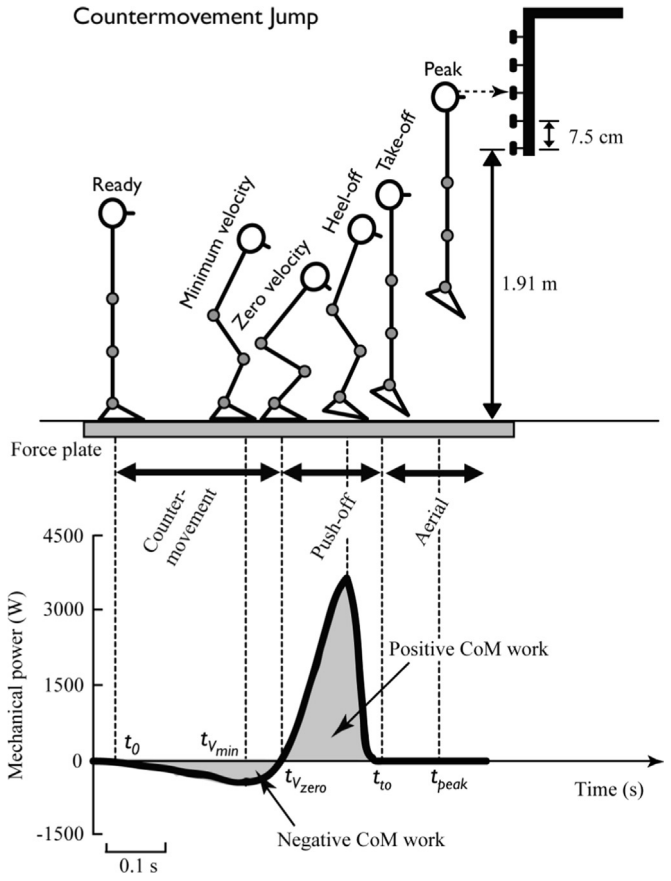

Fig. 1. Simplified steps in vertical jumping with countermovement. The countermovement jump (CMJ) consists of four sequential steps, including the countermovement, push-off, aerial, and landing (not shown in the figure). Negative CoM work is performed during the countermovement because of the lowering motion from standing upright to the zero velocity position, and positive work is performed during the push-off. The subjects were instructed to jump straight up to the five different levels marked on a ceiling pole, keeping their hands on their hips.

2. Methods

2.1. Experimental procedures

The kinematic and kinetic data (i.e., force–displacement curves) obtained from regular experimental trials (i.e., countermovement jumps) with ten healthy young subjects (10 males, mean age: 28 ± 2 yrs, mean height: 177 ± 5 cm, mean body mass: 70 ± 6 kg) who volunteered in this experiment were similar to one another and were categorized into two general types of countermovement jumps, depending on the curve shape (see the trajectories of subject-A and subject-B in figures; see details in the Appendix). In addition, the fundamental trajectory shapes were similar to the trajectory from a previously published paper (Linthorne, 2001); therefore, two representative samples (subject-A and subject-B) were selected and discussed throughout the paper (see averaged data for all subjects in the Appendix).

All the young subjects, including subject-A (male, age: 28 yr, height: 170 cm, body mass: 60 kg) and subject-B (male, age: 30 yr, height: 180 cm, body mass: 76 kg) with no leg injuries or history of balance disorder, participated in this study, after signing an informed consent form approved by the Institutional Review Board of the Korea Advanced Institute of Science and Technology (KAIST). The subjects were instructed to stand upright with their hands on their hips and to jump straight up to five different levels ranging from approximately 10% to 35% of their body heights. The highest level was nearly 92% of their maximum vertical jump heights, and the other levels were placed at equally spaced intervals of 7.5 cm. Black markers attached to a ceiling pole were used for vertical height guidance (Fig. 1). Each subject conducted five sets of five randomly ordered vertical elevations with a 1 min rest between each set. Before the data collection, the subjects rehearsed many pilot trials to become accustomed to reaching the target elevation.

2.2. Measurements

For each trial, the optical marker position, located at the sacrum (L5), and the ground reaction forces (GRFs) were recorded at a sampling rate of 200 Hz using motion capture cameras (Hawk®, Motion Analysis, US) and a forceplate (AccuGait®, AMTI, US). The vertical GRFs (F_{ver}) were integrated to estimate the velocity and position of the center of mass (CoM), with the sacral marker used to determine the integral constants (Kim and Park, 2011; Linthorne, 2001). The impulse-momentum method was then employed to calculate the take-off velocity of the CoM (V_{to}; Fig. 1; Eq. (1)) to estimate the vertical jump height (H_{peak}; Fig. 1; Eq. (2)) (Linthorne, 2001)

$$V_{to} = \frac{1}{M}\int_{t_0}^{t_{to}} (F_{ver} - Mg)\mathrm{d}t \tag{1}$$

$$H_{peak} = V_{to}(t_{peak} - t_{to}) - \frac{1}{2}g(t_{peak} - t_{to})^2 + CoM_{ver}(t_{to}) - CoM_{ver}(t_0) \tag{2}$$

where M, F_{ver}, g, and CoM_{ver} represent the body mass, vertical force, gravity, and vertical CoM displacement measured from the sacral marker, respectively. To ensure that the vertical jump heights were estimated accurately, the motion capture data were used to reconfirm the peak values as follows:

$$H_{peak} = CoM_{ver}(t_{peak}) - CoM_{ver}(t_0) \tag{3}$$

The optical marker positions and the GRFs were 5th-order Butterworth low-pass filtered with cut-off frequencies of 10 Hz for the motion capture data and 30 Hz for the forceplate data.

2.3. Fitting models to experimental data

To quantitatively understand the vertical force generation during the countermovement (i.e., while performing the negative work shown in Fig. 1) (Zelik and Kuo, 2012), the vertical force (F_{ver}) trajectories were curve-fitted using a combination of a semi-sinusoidal waveform (only the negative part of the sinusoidal wave)

and a linear increase, as follows:

$$F_{ver} = \begin{cases} MA\ \sin(2\pi\omega t) + Mg, & t \le 1/2\omega \\ Kt - K/2\omega + Mg, & t > 1/2\omega \end{cases} \quad (4)$$

where M, A, ω, K, g, and t represent the body mass, acceleration amplitude, frequency, time-derivative of force (=rate of force generation), gravity, and time relative to the event onset time, respectively, and the simulation ends when the time-integrals of the bottom equation are equal to the ones in the top equation (i.e., t_{Vzero}) (Eq. (4)). The semi-sinusoidal waveform described how each subject generated the maximum downward momentum during the early stage of countermovement, whereas the linear increase explained how the subject changed the direction of movement and gained force advantages at the beginning of push-off.

We determined the acceleration amplitude (A), frequency (ω), and time-derivative of force (K) from an optimization that minimized the least square error between the vertical GRF (F_{ver}) data and model simulation during the countermovement phase (Fig. 1). The optimization was performed by sequential quadratic programming (SQP) using a nonlinear equation solver (fminsearch, Matlab®), in which the initial conditions (A_{in}, ω_{in}, and K_{in}) were approximated from the experimental data (Fig. 1; Eq. (5))

$$\begin{cases} A_{in} = \min\{F_{ver}(t_0 : t_{V_{\min}})/M\} \\ \varpi_{in} = 1/2(t_{V_{\min}} - t_0) \\ K_{in} = (F_{ver}(t_{V_{zero}}) - F_{ver}(t_{V_{\min}}))/(t_{V_{zero}} - t_{V_{\min}}) \end{cases} \quad (5)$$

To determine whether the optimization found a global solution, we repeated the optimization multiple times over a wide range of random initial conditions (Kim et al., 2012; Kim and Park, 2011).

2.4. Inter-subject data comparison

First, vertical force vs. CoM displacement curves were plotted to illustrate the stiffness characteristics of the countermovement jump. Second, the amount of force and lowest CoM position at the start of push-off were plotted against the vertical jump height to verify the advantages of countermovement. Third, the downward momentum at the minimum velocity time (t_{Vmin}), the time-averaged resistive force, and the duration between the minimum velocity (t_{Vmin}) and zero velocity time (t_{Vzero}) were also plotted as functions of the vertical jump height to determine how the force advantages were obtained. Fourth, the model parameters (i.e., A, ω, and K) were examined as a function of the vertical jump height to quantify how each subject changed his jumping strategy across a wide range of vertical jump heights.

For inter-subject comparison (i.e., Subject-A vs. Subject-B), we normalized the CoM displacement and vertical jump height data by the body height (m), the force data by the body weight (N), the downward momentum data by the product of the body weight and the square root of the body height divided by the gravitational acceleration (kg m/s), and the time-derivative of the force data by the body weight multiplied by the square root of the gravitational acceleration divided by the body height (N/s). The significance of each of the reported trends from the parameter study was tested using regression analysis with a significance level of $p < 0.05$.

3. Results

3.1. Force–displacement curve during countermovement jump

The magnitude of the vertical CoM displacement scaled gradually with the vertical jump heights for both subjects, while the maximum vertical force was not significantly changed regardless of the vertical jump height (Fig. 2A and B). Even in the highest vertical jump, both subject-A and subject-B showed nearly constant peak values of vertical force compared with the values from their lowest jump ($p=0.19$). The vertical forces between the initial upright position and the minimum velocity position (V_{min}) were substantially smaller than the body weight and then drastically increased during the end of the countermovement (V_{zero}). This force reduction during the early stage of the countermovement was more clearly observed for subject-B, whereas the minimum velocity position (V_{min}) gradually decreased in both subjects as the vertical jump height increased.

3.2. Vertical force and CoM position at the start of push-off

The amount of force at the end of the countermovement (F_{cm}), which can be used as an additional force advantage for push-off, significantly increased with increasing vertical jump height ($p < 0.05$; Fig. 2A, B and C). Subject-A exhibited a smaller force advantage with greater scaling as the vertical jump height increased, whereas subject-B exhibited a larger force advantage but with lower scaling. The lowest CoM position (D_{cm}), just before starting the push-off, decreased with increasing vertical jump height (Fig. 2A, B and D). The slope of the regression line of the CoM position was steeper for subject-B, and the decreasing trends were statistically significant for both subjects ($p < 0.05$; Fig. 2D).

3.3. Downward momentum and resistive force

The magnitude of downward momentum at the minimum velocity position (V_{min}) increased with increasing vertical jump height (Fig. 3A), which means the difficulty of changing the direction of the CoM also increased. While linear scaling trends were clearly observed for both subjects, subject-B exhibited larger momentum with slightly greater scaling as the vertical jump height increased ($p < 0.05$). To change the vertical direction of the CoM from negative to positive, the time-averaged resistive force between the minimum velocity position (V_{min}) and the zero velocity position (V_{zero}) increased significantly with the vertical jump height ($p < 0.05$; Fig. 3B), while the duration did not show any scaling trend ($p=0.15$; Fig. 3C). Subject-A exhibited lower average forces but longer durations than subject-B.

3.4. Model simulation and parameter change

A simple curve-fit model with time-invariant, optimized model parameters (i.e., A, ω, and K) reproduced the force data of subject-A ($R^2=0.94\pm0.02$) and subject-B ($R^2=0.95\pm0.03$) reasonably well (Fig. 4). This model matched the data slightly better for the trials with vertical jump heights of intermediate elevation than the trials with the greatest heights because force reduction at the early stage of the countermovement was slightly distorted with increasing vertical jump height, making the semi-sinusoidal waveform less accurate in representing the distorted force data (Fig. 2A and B).

An increase in the absolute amplitude ($|A|$) and decrease in the frequency (ω) of the curve-fit model (i.e., semi-sinusoidal waveform) contributed to reaching a faster CoM velocity with increasing vertical jump height (Fig. 5A and B), resulting in an increase in the downward momentum (Fig. 3A). Subject-A changed the downward momentum by increasing the oscillation period ($1/\omega$) of the CoM acceleration with nearly constant amplitudes ($|A|$) ($p=0.62$), whereas subject-B changed the downward momentum by increasing both the acceleration amplitude and the oscillation period ($p < 0.05$). Subject-A exhibited a lower amplitude ($|A|$) across a range of vertical jump heights compared with subject-B; however, the periods ($1/\omega$) were slightly longer. Force advantages, which indicate the amount of vertical force greater than the body weight at the start of the push-off, were achieved by increasing the force generation per unit time (i.e., time-derivative of force, K) for both subjects ($p < 0.05$; Fig. 5C). Subject-B exhibited a nearly double magnitude but almost half the scaling rate compared with subject-A.

4. Discussion

4.1. Vertical jump strategies accommodating biomechanical constraints

A larger amount of force and longer duration, resulting in a higher vertical jump, can be achieved by appropriately selecting a countermovement strategy. Simply put, there are two options to increase the total amount of force: one is to increase the rate of force generation at a given time, and the other is to push off the

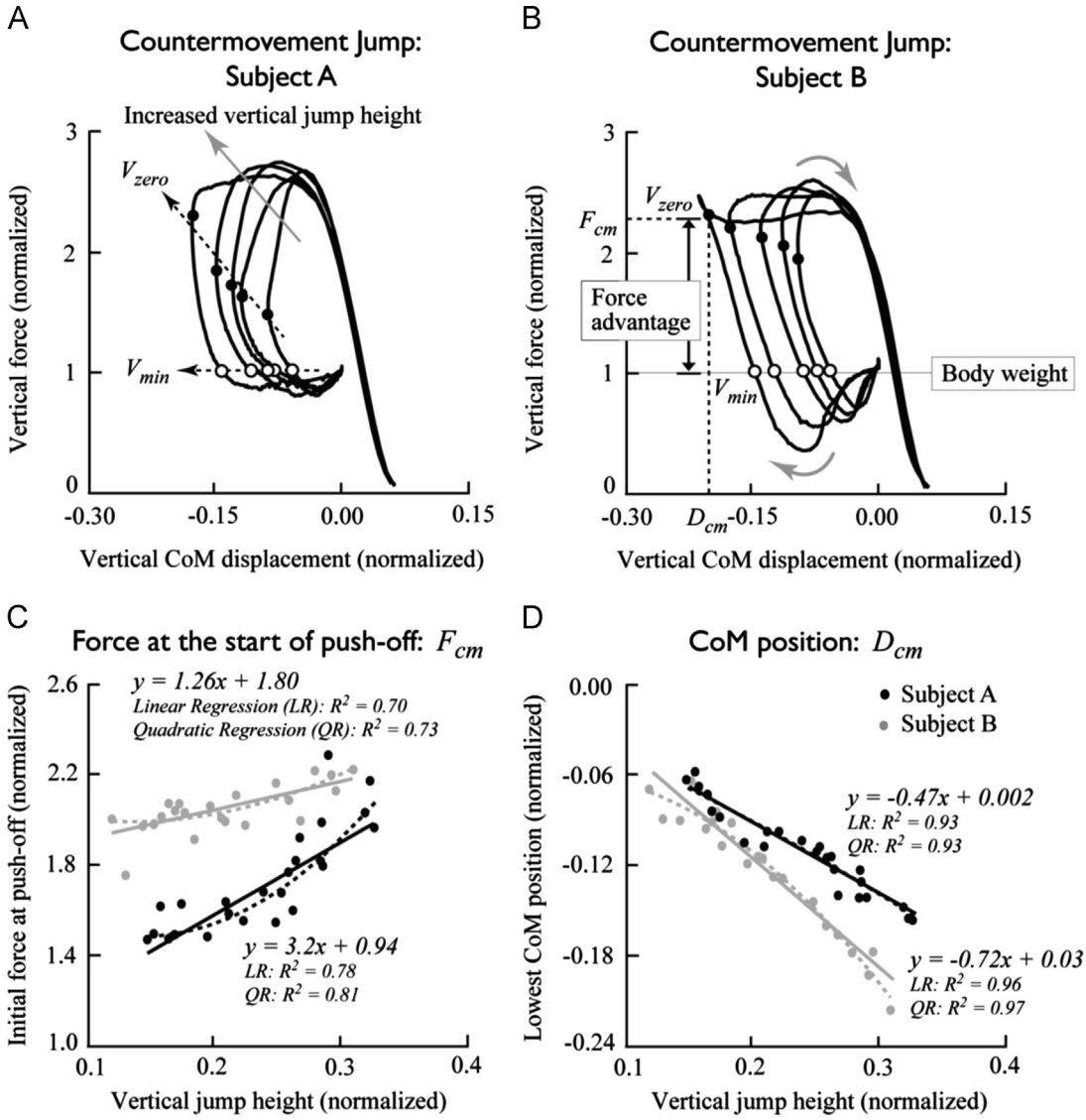

Fig. 2. (A and B) Average force–displacement curves of subject-A and subject-B during the countermovement jump. (C) The amount of vertical force and (D) the lowest CoM position at the start of push-off as a function of the vertical jump height. The vertical CoM displacements were defined based on the subject's standing position, with a negative sign for lowering. The solid circles and hollow circles in (A and B) indicate the zero velocity position and minimum velocity position, respectively, and the black dotted arrows indicate the scaling trends. The gray-colored arrow in (A) represents the extension of the trajectories with increasing vertical jump height, while the arrows in (B) represent the direction of change during the countermovement jump. The solid lines in (C and D) indicate the linear regression slopes of the empirical data for each subject as a function of the vertical jump height. The full equations for the curve fits are displayed in the form of $y=ax+b$, with the goodness of fit data, while quadratic regressions (dotted lines) are also used to best fit the data in all figures and regressions. These simple functions were chosen to describe the data trend based on the Akaike Information Criterion. The normalization methods are described in the METHODS section.

ground with the help of an initial vertical force (i.e., force advantage) when first rising. Because the rate of force generation in muscle is limited due to biomechanical constraints (Fig. 6), we thought that the subjects would be required to select the latter method to increase the vertical jump height using the countermovement. Force reduction during the early stage of the countermovement, by abruptly lowering the CoM position (Fig. 5A and B), can create momentum toward the ground (Fig. 3A), which will be compensated by generating a resistive force over a short time (Fig. 3B, C and Fig. 5C). This upward force at the end of the countermovement (i.e., zero velocity position) can contribute to the increase in the total amount of vertical force during the push-off (i.e., positive CoM work) (Fig. 2A, B and C), increasing the vertical jump height. In addition, a longer duration for increasing the force supply can be achieved by simply lowering the CoM position (Fig. 2A, B and D), which yields larger joint deviations from the initial upright posture.

The force-displacement curves obtained from the empirical data and virtual data can be used to better understand the jumping strategy for the higher elevation (Fig. 6). Assuming that all pathways, including the boundary points P_1 (indicating lack of "increasing force advantage" and "lowering CoM"), P_2 (indicating lack of "increasing force advantage"), and P_3, which are located at the end of the negative work trajectories, perform the same amount of positive work, the vertical jump height is the same for all three cases. However, the subjects have no choice other than to reach point P_3 because of the limited amount of peak force and/or the limited rate of force generation, i.e., it takes a certain amount of time and distance for joint extension to attain a high level of force.

The subjects are aware that body dynamics are being subjected to various jump heights and may select appropriate jumping strategies that satisfy feasible force constraints. Although there may be multiple options for changes in the boundary points on the

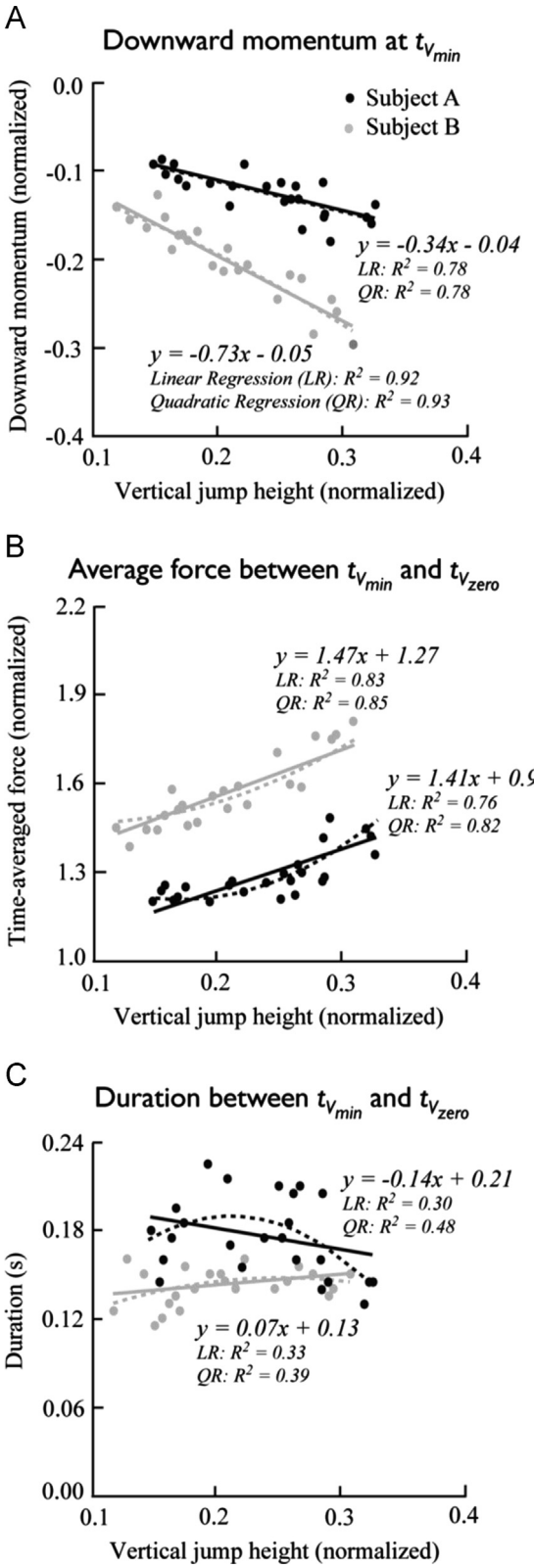

Fig. 3. (A) Downward momentum at the minimum velocity position, (B) time-averaged force between the minimum- and zero-velocity positions, and (C) its duration at the corresponding vertical jump heights. The solid lines indicate the linear regression slopes for each subject.

force–displacement curve as the vertical jump height increases, empirical data have shown that the boundary points continuously, as well as progressively, moved toward the left with an upward

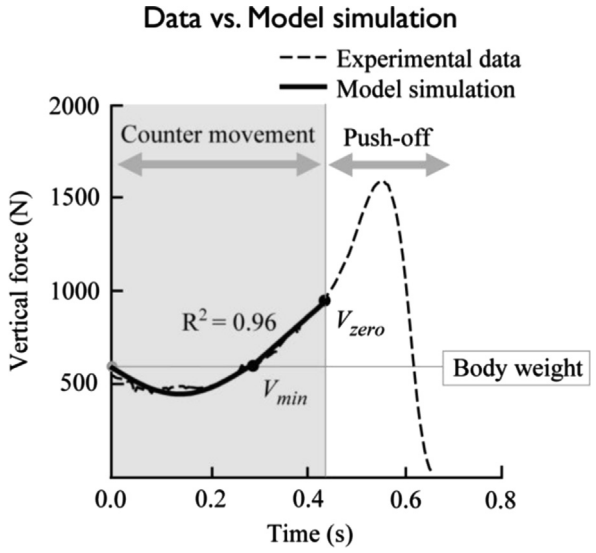

Fig. 4. A representative data-fitting result: the vertical force data (dotted line) for the 48-cm vertical elevation were fitted with a combination of a semi-sinusoidal waveform and a linear increase (solid line). The R^2 value obtained by comparing the data with the simulation was 0.96.

bend, not discretely or irregularly (Fig. 2A and B). Thus, the subjects gradually changed their countermovement strategy as the biomechanical constraints became increasingly constraining without exceeding the maximum allowable force. These gradual changes in the boundary points, which are determined directly from the model parameters (i.e., A, ω, and K), are also related to the fact that the changes of model parameters with vertical jump height could be described by simple linear or quadratic functions, which implies potential regularities in choosing the countermovement strategy (i.e., employing jump strategies orderly with being aware of body dynamics).

4.2. Boundary points that describe the countermovement jump strategy

The boundary points (P_1, P_2, and P_3 in Fig. 6) on the force–displacement curve can be used to describe the strategy of the countermovement jump, where the points are determined from the model parameters (i.e., A, ω, and K). The boundary points are located between two trajectories of countermovement and push-off, which indicates that the points are the outcomes of the negative CoM work and serve as seed forces for the positive CoM work. Because the peak forces appear to be nearly constant across the range of vertical jump heights (consistent with the observation that the amount of peak vertical forces did not differ between maximal and submaximal squat jumps) (Van Zandwijk et al., 2000), the push-off trajectory on the force–displacement curve has a certain degree of predictability. In other words, once the boundary points have been determined, it might be possible to roughly derive the rest of the information regarding how the positive CoM work was performed. Thus, we thought that the boundary points might represent the characteristics of each countermovement jump.

Changes in the boundary points on the force–displacement curve could describe changes in the strategy of the countermovement jump. For example, subject-A showed gradual scaling of the boundary points with increased vertical jump height toward the left with a distinct upward bend (Fig. 2A), while subject-B showed lower scaling but with much larger force advantages, even for the lowest jump (Fig. 2B). This result might be related to the subjects' preferential use of different jump strategies, where the strategies

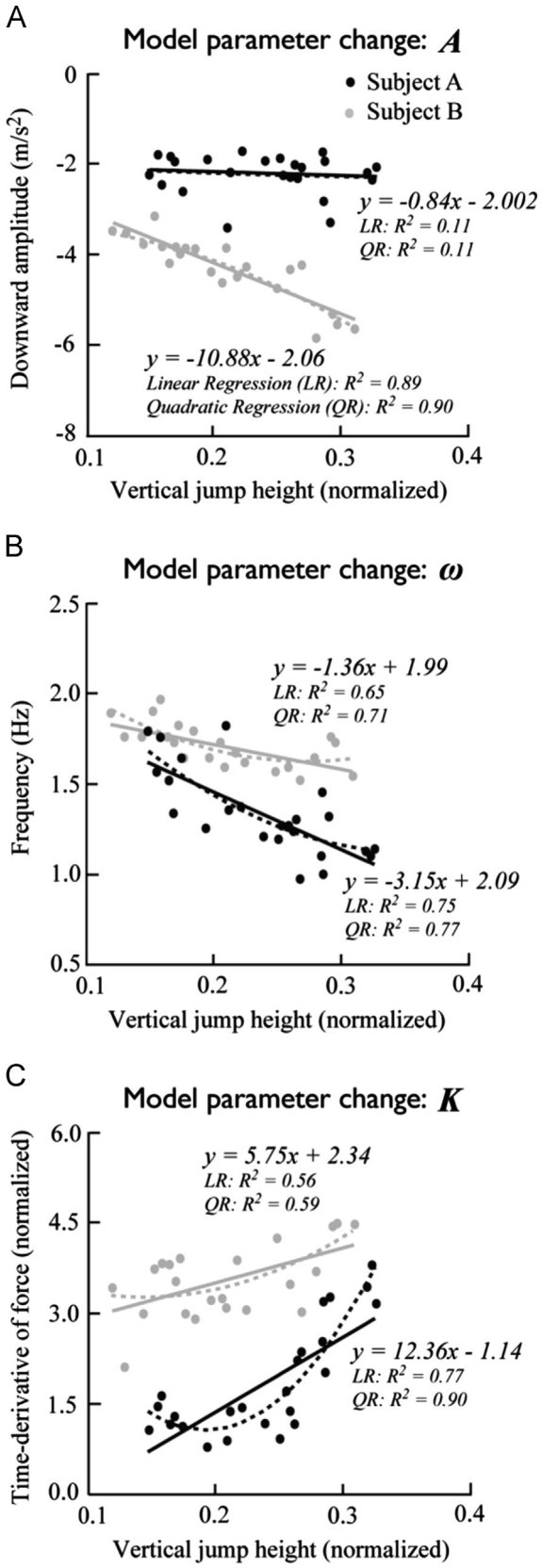

Fig. 5. Curve-fit model parameters: for each subject, the (A) acceleration amplitude, (B) frequency, and (C) time-derivative of force as a function of the vertical jump height. The solid lines indicate the linear regression slopes.

could be quantified using the regression slope and the magnitude of the model parameters because the boundary points are derived from those parameters: the oscillation amplitude and the frequency

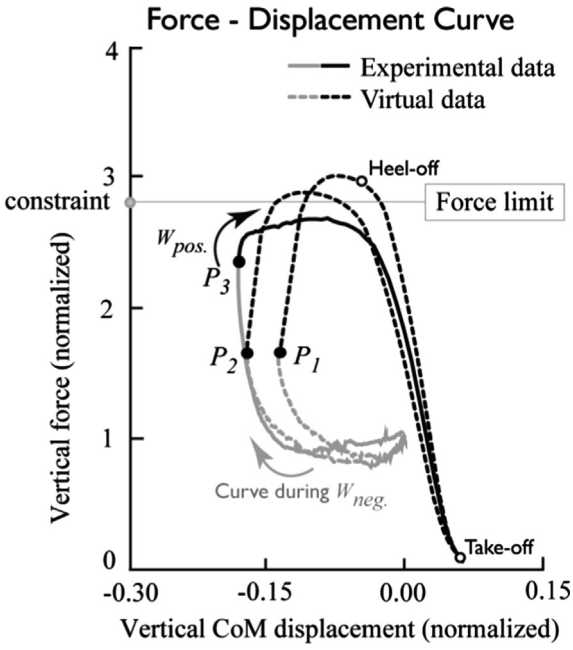

Fig. 6. Force–displacement curves of subject-A (solid lines) and virtual curves (dotted lines). The trajectory that corresponds to the highest vertical jump height was selected from Fig. 2A, and the virtual curves were assumed to have the same vertical jump height, which indicates that the areas under the black colored lines are exactly the same. The black solid circles (P_1, P_2, and P_3) represent the boundary points between the curves for performing negative work (gray) and positive work (black) during the countermovement jump, while the hollow circles represent the heel-off and take-off phases. The arrows indicate the direction of change.

of the CoM quantitatively describe how downward momentum (i.e., force reduction) is achieved, and the rate of force generation describes how resistive force creates an additional force advantage (i.e., force propulsion) to support the push-off.

4.3. Model limitations

Because multi-joint characteristics were grouped into the simple CoM mechanics, the current model does not specify how each joint contributed to the changes in boundary points (or jumping strategy). Therefore, we did not attempt to expand our findings from the simple descriptive model to multi-joint mechanics and also did not discuss how the model parameters could be mapped onto muscle physiology in a direct way. However, the simple model can quantify the countermovement with only a limited number of model parameters from the perspective of CoM mechanics (i.e., force reduction and propulsion), which may be used to describe the countermovement strategy.

Conflict of interest statement

None.

Acknowledgments

This research was supported by the Korea Advanced Institute of Science and Technology (KAIST), the National Research Foundation of Korea (NRF), and the Korea Institute of Machinery & Materials (KIMM).

Appendix A. Supporting information

Supplementary data associated with this article can be found in the online version at http://dx.doi.org/10.1016/j.jbiomech.2014.06.013.

References

Anderson, F.C., Pandy, M.G., 1993. Storage and utilization of elastic strain energy during jumping. J. Biomechan. 26, 1413–1427.

Arakawa, H., Nagano, A., Hay, D.C., Kanehisa, H., 2013. The effects of ankle restriction on the multijoint coordination of vertical jumping. J. Appl. Biomech. 29, 468–473.

Bobbert, M.F., Gerritsen, K.G., Litjens, M.C., Van Soest, A.J., 1996. Why is countermovement jump height greater than squat jump height? Med. Sci. Sports Exercise 28, 1402–1412.

Domire, Z.J., Challis, J.H., 2007. The influence of squat depth on maximal vertical jump performance. J. Sports Sci. 25, 193–200.

Horak, F.B., Nashner, L.M., 1986. Central programming of postural movements: adaptation to altered support-surface configurations. J. Neurophysiol. 55, 1369–1381.

Kim, S., Atkeson, C.G., Park, S., 2012. Perturbation-dependent selection of postural feedback gain and its scaling. J. Biomechan. 45, 1379–1386.

Kim, S., Park, S., 2011. Leg stiffness increases with speed to modulate gait frequency and propulsion energy. J. Biomechan. 44, 1253–1258.

Komi, P.V., 2000. Stretch-shortening cycle: a powerful model to study normal and fatigued muscle. J. Biomechan. 33, 1197–1206.

Lees, A., Vanrenterghem, J., De Clercq, D., 2006. The energetics and benefit of an arm swing in submaximal and maximal vertical jump performance. J. Sports Sci. 24, 51–57.

Linthorne, N.P., 2001. Analysis of standing vertical jumps using a force platform. Am. J. Phys. 69, 1198–1204.

McLellan, C.P., Lovell, D.I., Gass, G.C., 2011. The role of rate of force development on vertical jump performance. J. Strength Cond. Res. 25, 379–385.

Park, S., Horak, F.B., Kuo, A.D., 2004. Postural feedback responses scale with biomechanical constraints in human standing. Exp. Brain Res. 154, 417–427.

Svantesson, U., Ernstoff, B., Bergh, P., Grimby, G., 1991. Use of a Kin-Com dynamometer to study the stretch-shortening cycle during plantar flexion. Eur. J. Appl. Physiol. Occup. Physiol. 62, 415–419.

Van Schenau, G.J.I., Bobbert, M.F., De Haan, A., 1997. Does elastic energy enhance work and efficiency in the stretch-shortening cycle? J. Applied Biomechan. 13, 389–496.

Van Zandwijk, J., Bobbert, M.F., Munneke, M., Pas, P., 2000. Control of maximal and submaximal vertical jumps. Med. Sci. Sports Exerc. 32, 477–485.

Vanrenterghem, J., Lees, A., De Clercq, D., 2008. Effect of forward trunk inclination on joint power output in vertical jumping. J. Strength Cond. Res. 22, 708–714.

Zelik, K.E., Kuo, A.D., 2012. Mechanical work as an indirect measure of subjective costs influencing human movement. PLoS One 7, e31143.